

# Consistency of Perfect Fluidity and Jet Quenching in semi-Quark-Gluon Monopole Plasmas

Jiechen Xu,<sup>1,\*</sup> Jinfeng Liao,<sup>2,3,†</sup> and Miklos Gyulassy<sup>1,‡</sup>

<sup>1</sup>*Department of Physics, Columbia University, 538 West 120th Street, New York, NY 10027, USA*

<sup>2</sup>*Physics Dept and CEEM, Indiana University, 2401 N Milo B. Sampson Lane, Bloomington, IN 47408, USA*

<sup>3</sup>*RIKEN BNL Research Center, Bldg. 510A, Brookhaven National Laboratory, Upton, NY 11973, USA*

(Dated: April 2, 2015)

We utilize a new framework, CUJET3.0, to deduce the energy and temperature dependence of jet transport parameter,  $\hat{q}(E > 10 \text{ GeV}, T)$ , from a combined analysis of available data on nuclear modification factor and azimuthal asymmetries from RHIC/BNL and LHC/CERN on high energy nuclear collisions. Extending a previous perturbative-QCD based jet energy loss model (known as CUJET2.0) with (2+1)D viscous hydrodynamic bulk evolution, this new framework includes three novel features of nonperturbative physics origin: (1) the Polyakov loop suppression of color-electric scattering (aka “semi-QGP” of Pisarski et al) and (2) the enhancement of jet scattering due to emergent magnetic monopoles near  $T_c$  (aka “magnetic scenario” of Liao and Shuryak) and (3) thermodynamic properties constrained by lattice QCD data. CUJET3.0 reduces to v2.0 at high temperatures  $T > 400 \text{ MeV}$ , but greatly enhances  $\hat{q}$  near the QCD deconfinement transition temperature range. This enhancement accounts well for the observed elliptic harmonics of jets with  $p_T > 10 \text{ GeV}$ . Extrapolating our data-constrained  $\hat{q}$  down to thermal energy scales,  $E \sim 2 \text{ GeV}$ , we find for the first time a remarkable consistency between high energy jet quenching and bulk perfect fluidity with  $\eta/s \sim T^3/\hat{q} \sim 0.1$  near  $T_c$ .

PACS numbers: 25.75.-q, 12.38.Mh, 24.85.+p, 13.87.-a

*Introduction.*— Deconfined quark-gluon plasmas (QGP) are created in ultrarelativistic heavy-ion collisions at the BNL Relativistic Heavy Ion Collider (RHIC) and the CERN Large Hadron Collider (LHC) [1–3]. Two of the most striking properties of the QGP are its perfect (minimally viscous) fluidity as quantified by its shear viscosity to entropy density ratio  $\eta/s \sim 0.1 - 0.2$  [4–8] and the strong quenching of high energy jets quantified by the normalized jet transport coefficient  $\hat{q}/T^3$  [10–15, 21]. Interestingly by comparing RHIC and LHC measurements it was found that both QGP properties vary with beam energy with extracted average  $\eta/s$  increasing while  $\hat{q}/T^3$  decreasing (by  $\sim 30\%$ ) from RHIC to LHC [7–10, 17–19]. These observations indicate a relatively strong temperature dependence of such medium properties in the  $1 \sim 3T_c$  region.

Up to now however has been no quantitative and consistent microscopic understanding of both bulk collectivity and jet quenching in QGP. Perturbative-QCD (pQCD) based models for  $\hat{q}(E, T)$  that account for jet quenching at high energies are found to be inconsistent with small  $\eta/s \sim T^3/\hat{q}$  when extrapolated down to thermal energy scales [6]. On the other hand, strong coupling models that can easily account for  $\eta/s \sim 1/4\pi$  perfect fluidity tend to over-predict quenching of high energy jets when extrapolated to high energies [20, 21]. None of these models show strong T-dependence for  $\eta/s$  or  $\hat{q}/T^3$ .

In this Letter, we address these questions by taking into account three important nonperturbative properties of QGP suggested by lattice QCD calculations into a new microscopic model of *semi-quark-gluon monopole plasmas* (sQGMP) in the crossover QCD transition tem-

perature range  $T \sim 1 - 2 T_c$ : (1) the lattice Polyakov loop suppresses color-electric degrees of freedom (aka the “semi-QGP” [22–25]) and (2) lattice data on color magnetic degrees of freedom suggests the emergence of color-magnetic monopoles near  $T_c$  (aka “magnetic scenario” [26–28]). In addition (3) lattice data on the QCD equation state [29, 30],  $P(T)$  and  $S(T) = dP/dT$ , shows a rapid decrease as  $T$  decreases, limiting the sum of color electric (q+g) and color magnetic (m) densities. No arbitrary parameters are introduced as these new features are fully constrained by lattice QCD data [31–37].

In order to demonstrate these, we generalize the pQCD-based CUJET2.0 scheme for jet energy loss  $dE/dx$ , to include effects of (1) suppressed semi-QGP color electric degrees of freedom (reducing  $dE_{q+g}/dx$ ) and (2) enhanced  $dE_m/dx$  of jets on emergent color magnetic monopoles near  $T_c$ . We find that the resulting  $\hat{q}(E, T)$  dependence on jet energy  $E$ , and sQGMP temperature  $T$ , is such that when extrapolated down to thermal energy scale  $E < 2 \text{ GeV}$  near  $T_c$ , it is greatly enhanced so that our predicted bulk  $\eta/s \approx T^3/\hat{q}$  falls close to minimal uncertainty bound near  $T_c$ . We thus confirm quantitatively with CUJET3.0 the early qualitative suggestions [26–28, 38–44], namely the key microscopic dynamical ingredient that can reconcile observed low  $p_T$  bulk perfect fluidity with high  $p_T$  perturbative QCD jet quenching, is the emergence of color magnetic degrees of freedom. The new twist with CUJET3.0 is the essential role of semi-QGP suppression of color electric degrees of freedom. It is the combination of these two novel effects in our extended picture of semi-quark-gluon-monopole plasmas that can give rise to both hard

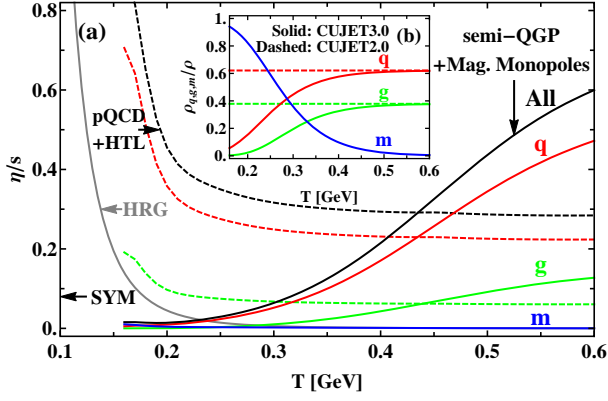


FIG. 1. (Color online) (a) Temperature dependence of shear viscosity per entropy density ( $\eta/s$ ) for quasi-partons of quark (q), gluon (g) and monopole (m) type, as well as their overall contribution (All). (b) The density fractions of q, g, m. Solid lines correspond to the sQGMP model (CUJET3.0), while dashed ones correspond to the pQCD+HTL model (CUJET2.0). The AdS/CFT perfect fluidity limit  $\eta/s = 1/4\pi$  is marked as SYM. The shaded line is the Hadron Resonance Gas (HRG)  $\eta/s$  from [82]. The falling of sQGMP's  $\eta/s$  below  $1/4\pi$  is due to the limitation of kinetic theory estimate of  $\eta/s$  in the low  $E$  extrapolation of  $T^3/\hat{q}(E \sim 3T, T)$  [6].

and soft transport properties of the new phase of QCD matter produced in ultra-relativistic heavy ion collisions.

Leaving detailed comparison with data to later, we highlight first the two main findings from our sQGMP model. For the shear viscosity  $\eta/s$ , we show in Fig.1 the results from two models: the CUJET2.0 result assuming the pQCD HTL model of QGP compared to the CUJET3.0 result based on the sQGMP model. The former perturbative model clearly over-predicts the phenomenologically deduced  $\eta/s$  and has the wrong sign of temperature trend from RHIC to LHC. On the other hand, the nonperturbative sQGMP model features an especially small value  $\eta/s \sim 0.1$  in  $T \lesssim 2T_c$  range, with a rapid increase toward high  $T$ , in line with empirical data. Our main point is that sQGMP provides a viable path toward perfect fluidity in contrast to all past attempts starting from perturbative jet quenching as considered in the JET collaboration summary [10].

The jet transport coefficients  $\hat{q}/T^3$  of the same two models are shown in Fig.2. Here one sees the strong near- $T_c$  enhancement of the sQGMP opacity as compared with the perturbative HTL model of the QGP. As we will demonstrate in Fig.4 later, while both models of the QGP can describe the single inclusive hadron suppression (quantified by nuclear modification factor  $R_{AA}$ ) data, only the nonperturbative sQGMP model with non-trivial near- $T_c$  behavior can account well for both high  $p_T$   $R_{AA}$  and its azimuthal anisotropy  $v_2$ . We again emphasize that no new parameters are introduced in this analysis since the sQGMP properties are constrained by available lattice QCD data — see details in Fig.3.

*The sQGMP model setup.*— Let us start with a brief

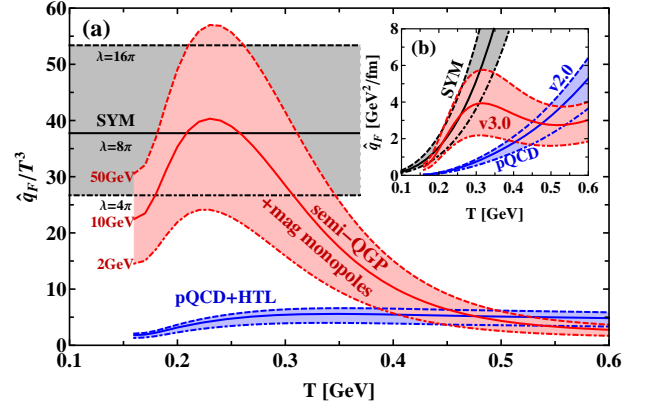


FIG. 2. (Color online) Temperature dependence of (a) the dimensionless jet transport coefficient  $\hat{q}/T^3$  and (b) the absolute  $\hat{q}$  for a quark jet ( $F$ ) with initial energy  $E = 2, 10, 50$  GeV, computed from CUJET3.0 (semi-QGP + chromomagnetic monopoles) with  $(\alpha_c, c_m) = (0.95, 0.3)$ , compared with the result from CUJET2.0 (pQCD + HTL) [45] with  $(\alpha_{max}, f_E, f_M) = (0.39, 1, 0)$ , and the result from  $N = 4$  super Yang-Mills (SYM) calculations ( $\hat{q} \approx 26.69\sqrt{\lambda/4\pi}T^3$ ) [46].

discussion on the previous CUJET2.0 framework. In the radiative energy loss sector, the perturbative QCD (pQCD) based  $n = 1$  DGLV [47–49] opacity series with multi-scale running strong couplings [50, 51] and Hard Thermal Loop (HTL) dynamical screening potential [52] can be written as [45]:

$$x_E \frac{dN_g^{n=1}}{dx_E} = \frac{18C_R}{\pi^2} \frac{4 + N_f}{16 + 9N_f} \int d\tau n(\mathbf{z}) \Gamma(\mathbf{z}) \int d^2k \times \alpha_s \left( \frac{\mathbf{k}^2}{x_+(1-x_+)} \right) \int d^2q \frac{\alpha_s^2(\mathbf{q}^2)}{\mu^2(\mathbf{z})} \frac{f_E^2 \mu^2(\mathbf{z})}{\mathbf{q}^2(\mathbf{q}^2 + f_E^2 \mu^2(\mathbf{z}))} \times \frac{-2(\mathbf{k} - \mathbf{q})}{(\mathbf{k} - \mathbf{q})^2 + \chi^2(\mathbf{z})} \left[ \frac{\mathbf{k}}{\mathbf{k}^2 + \chi^2(\mathbf{z})} - \frac{(\mathbf{k} - \mathbf{q})}{(\mathbf{k} - \mathbf{q})^2 + \chi^2(\mathbf{z})} \right] \times \left[ 1 - \cos \left( \frac{(\mathbf{k} - \mathbf{q})^2 + \chi^2(\mathbf{z})}{2x_+ E} \tau \right) \right] \left( \frac{x_E}{x_+} \right) \left| \frac{dx_+}{dx_E} \right|. \quad (1)$$

In the above  $C_R = 4/3$  (quark), 3 (gluon) is the quadratic Casimir of the jet;  $\mathbf{z} = (x_0 + \tau \cos \phi, y_0 + \tau \sin \phi; \tau)$  is the coordinate of the jet in the transverse plane;  $n(\mathbf{z})$  and  $T(\mathbf{z})$  is the local number density and temperature of the medium in the local rest frame. In the presence of hydrodynamical four velocity fields,  $u_f^\mu(z)$ , a relativistic flow correction factor  $\Gamma(\mathbf{z}) = u_f^\mu n_\mu$  must also be taken into account [20, 53, 54], with flow velocity  $u_f^\mu = \gamma_f(1, \vec{\beta}_f)$  and null parton velocity  $n^\mu = (1, \vec{\beta}_{jet})$ . The Debye screening mass  $\mu(\mathbf{z})$  is determined from solving the self-consistent equation  $\mu^2(\mathbf{z}) = \sqrt{4\pi\alpha_s(\mu^2(\mathbf{z}))T(\mathbf{z})\sqrt{1 + N_f/6}}$  as in [55];  $\chi^2(\mathbf{z}) = M^2 x_+^2 + m_g^2(\mathbf{z})(1-x_+)$  controls the Landau-Pomeranchuk-Migdal (LPM) phase, the gluon plasmon mass  $m_g^2(\mathbf{z}) = f_E^2 \mu^2(\mathbf{z})/2$ , and  $f_E$  is the HTL deformation parameter. The gluon fractional energy  $x_E$  and fractional plus-momentum  $x_+$  are related via  $x_+(x_E) = x_E[1 + \sqrt{1 - (k_\perp/x_E E)^2}]/2$ .

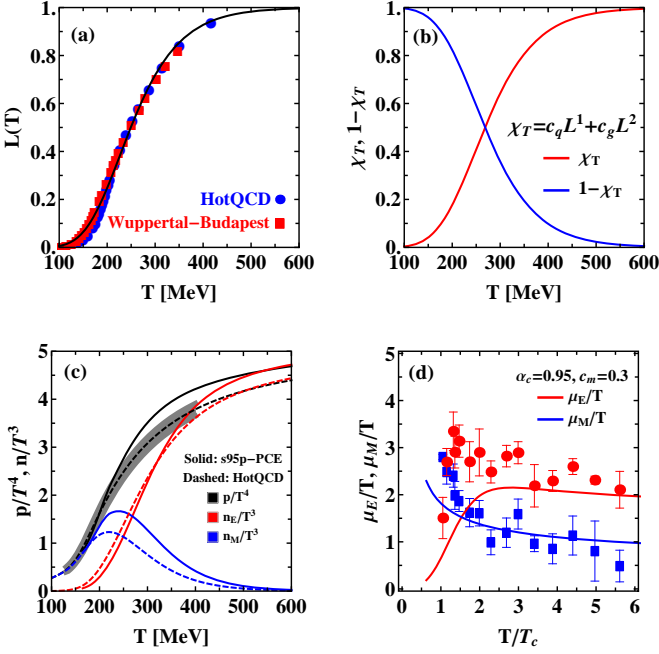


FIG. 3. (Color online) (a) The Polyakov loop  $L(T)$  parametrization in the sQGMP model compared with lattice data from HotQCD [58] and Wuppertal-Budapest Collaboration [59]; (b) The fractions of electric (red,  $\chi(T)$ ) and magnetic (blue,  $1 - \chi(T)$ ) quasi-particles in sQGMP as temperature varies. (c) The EOS from HotQCD (gray band: lattice data, dashed black: parametrization, both are in [30]) as well as the number density of E (red) and M (blue) degrees of freedom at various temperatures. (d) The temperature dependence of the screening mass  $\mu_E/T$  (red, electric) and  $\mu_M/T$  (blue, magnetic) in sQGMP compared with lattice calculations [60].

A key ingredient in Eq. (1) is the scattering rate of jet partons by medium scattering centers, given by

$$x \frac{dN}{dx} \propto \dots \int_{q^2} \left[ \frac{n \alpha_s^2(q^2) f_E^2}{q^2(q^2 + f_E^2 \mu^2)} \right] \dots \quad (2)$$

With both electric and magnetic quasiparticles in sQGMP, the above integrand needs to be generalized as:

$$\left[ \frac{n_e (\alpha_s(q^2) \alpha_s(q^2)) f_E^2}{q^2(q^2 + f_E^2 \mu^2)} + \frac{n_m (\alpha^e(q^2) \alpha^m(q^2)) f_M^2}{q^2(q^2 + f_M^2 \mu^2)} \right] \quad (3)$$

And in the above  $\alpha^e \alpha^m = 1$  at any scale according to Dirac quantization condition [27]. The parameters  $f_E$  and  $f_M$  are defined as  $f_E = \mu_E/\mu$  and  $f_M = \mu_M/\mu$  with  $\mu_E$  and  $\mu_M$  the electric and magnetic screening masses respectively. We further divide the total scattering center density  $n$  into electric ones with fraction  $\chi_T = n_e/n$  and thus magnetic ones with fraction  $1 - \chi_T = n_m/n$ . Expression (3) then reads:

$$n \left[ \alpha_s^2 \chi_T \left( f_E^2 + \frac{f_E^2 f_M^2 \mu^2}{q^2} \right) + (1 - \chi_T) \left( f_M^2 + \frac{f_E^2 f_M^2 \mu^2}{q^2} \right) \right] \quad (4)$$

In the regime  $T \sim T_c$  the running of the strong coupling becomes non-perturbative [26, 27, 56, 57] and poorly un-

derstood. A plausible parametrization, motivated by extraction [27] from lattice data, is given by:

$$\alpha_s(Q^2) = \alpha_c / \left[ 1 + \frac{9\alpha_c}{4\pi} \text{Log}\left(\frac{Q^2}{T_c^2}\right) \right], \quad (5)$$

with  $T_c = 160$  MeV. At large  $Q^2$ , Eq. (5) converges to vacuum running, while at  $Q = T_c$ , the  $\alpha_s$  reaches  $\alpha_c$ .

To determine  $\chi_T$ , we notice: (1) at high  $T$  it should go to unity  $\chi_T \rightarrow 1$ ; (2) getting close to the regime  $T \sim (1 - 3)T_c$  the Polyakov loop value  $L$  deviates significantly from unity, implying suppression  $\sim L$  for quarks and  $\sim L^2$  for gluons. Such near- $T_c$  suppression, as first emphasized in the “semi-QGP” model [22–25], implies that quark and gluon densities drop much faster than the thermodynamic quantities: see Fig.3c. This points to “missing” degrees of freedom, identified as thermal monopoles [26, 27] that are strongly enhanced near- $T_c$ . Such monopoles emerge in gauge theories at strong coupling and are thermal excitations of magnetic condensate as the “dual superconductor” enforcing vacuum confinement [31–33]. With such insights we adopt the ansatz:

$$\chi_T = c_q L + c_g L^2, \quad (6)$$

where we use the Stefan Boltzmann (SB) fraction coefficient for quarks and gluons,  $c_q = (10.5N_f)/(10.5N_f + 16)$  and  $c_g = 16/(10.5N_f + 16)$ . The temperature dependent Polyakov loop  $L(T)$  can be parametrized from lattice data ( $T$  in GeV) as  $L(T) = \left[ \frac{1}{2} + \frac{1}{2} \text{Tanh}[7.69(T - 0.0726)] \right]^{10}$ . Both the HotQCD [58] and Wuppertal-Budapest [59] results are well-fitted (see Fig.3(a)) thus fixing  $\chi_T$  and  $(1 - \chi_T)$  in Fig.3(b).

The electric and magnetic screening masses ( $\mu_{E,M} = f_{E,M} \mu$ ) also play important roles. To specify these, we draw upon insights from very high temperature limit where one expects  $f_E \rightarrow 1$  from HTL results and  $f_M \sim g$  (i.e.  $\mu_M \sim g^2 T$ ) from magnetic scaling in high  $T$  dimensional reduction. On general grounds the screening masses are expected to scale as  $\mu_{E,M}^2 \sim \alpha_{E,M} n_{E,M}/T$ . Therefore in extrapolation to lower temperature we expect the electric mass to be suppressed like  $\sqrt{\chi_T(T)}$  but approaching unity at high  $T$  limit. For the magnetic screening mass, we have  $n_M \sim (\alpha_E T)^3$ , i.e.  $\mu_M \sim \alpha_E T$  (as supported by lattice [60]). Thus we use the following  $T$ -dependent screening masses in the model:

$$f_E(T) = \sqrt{\chi_T} \quad , \quad f_M(T) = c_m g \quad . \quad (7)$$

For the consistency with Eq. (1), the “coupling” is defined via  $g(T) = \sqrt{4\pi\alpha_s(\mu^2(T))} = \mu(T)/(T\sqrt{1 + N_f/6})$ . These masses are in reasonable agreement with lattice extracted values [60]: see Fig.3(d).

In the CUJET3.0 framework, the bulk evolution profiles are generated from the VISH2+1 [7, 8, 29] code with MC-Glauber initial condition,  $\tau_0 = 0.6$  fm/c, s95p-PCE Equation of State (EOS),  $\eta/s = 0.08$ , and Cooper-Frye freeze-out temperature 120 MeV. Event-averaged

smooth profiles are embedded, and the path integrations in Eq. (1) for jets initially produced at various transverse coordinates are cutoff at dynamical  $T(\mathbf{x}_0, \phi, \tau)|_{\tau_{max}} = 160$  MeV hypersurfaces. All these bulk evolution details are the same as those in the CUJET2.0 framework [45].

Poisson multiple gluon emissions are assumed, and Gaussian fluctuations for elastic energy loss (Thoma-Gyulassy, c.f. [61]) are taken into account. The total energy loss probability distribution is the convolution of radiative and elastic sector; it is then convoluted with LO pQCD (light) [62] or FONLL (heavy) [63] pp production spectra, Glauber A+A initial jet distributions [64], and finally jet fragmentation functions [65, 66] to get the nuclear modification of hadron spectra in A+A collisions.

*Jet quenching phenomenology from CUJET3.0.*— We now apply this new framework for computing high  $p_T$  single inclusive hadron observables. The nuclear modification factor  $R_{AA}^h$  for hadron species  $h$  is defined as the ratio of the A+A spectrum to the p+p spectrum, scaled according to the number of binary collisions  $N_{bin}$ :  $R_{AA}^h(p_T, y; \sqrt{s}, b) = \frac{dN_{AA}^h/dydp_T}{N_{bin} dN_{pp}^h/dydp_T}$ . The azimuth-differential yield  $\frac{dN^h}{dydp_T d\phi}$  can be quantified by its Fourier component coefficients  $v_n$ :  $\frac{dN^h}{dydp_T d\phi}(p_T, \phi, y; \sqrt{s}, b) = \frac{1}{2\pi} \frac{dN^h}{dydp_T} \times [1 + 2 \sum_{n=1}^{\infty} v_n^h \cos(n(\phi - \Psi_n^h))]$ . We focus on the second, elliptic moment  $v_2$  at high  $p_T$ .

Fig. 4 shows the comparison of data and CUJET3.0 results for mid-rapidity ( $y = 0$ )  $R_{AA}(p_T)$  and  $v_2(p_T)$  of inclusive neutral pions ( $\pi^0$ ) and charged particles ( $h^\pm$ ) in Au+Au  $\sqrt{s_{NN}} = 200$  GeV and Pb+Pb  $\sqrt{s_{NN}} = 2.76$  TeV semi-peripheral collisions. There is only one parameter  $\alpha_c$  that is fixed by a single reference data point, i.e.  $R_{AA}^{h^\pm}(p_T = 12.5 \text{ GeV}) \approx 0.3$  at LHC, and all other parameters are already determined from lattice QCD (including the  $c_m$  in Eq. (7), c.f. Fig.3). Evidently, the CUJET3.0 framework simultaneously describes *both*  $R_{AA}$  and  $v_2$  at *both* RHIC and LHC. This finding quantitatively validates earlier arguments [41, 54] that enhanced energy loss at later time generically increases  $v_2$  for fixed  $R_{AA}$ .

We also predict the high  $p_T$   $R_{AA}(p_T)$  and  $v_2(p_T)$  for D and B meson at LHC semi-peripheral 20-30% Pb+Pb  $\sqrt{s_{NN}} = 2.76$  TeV collisions, shown in Fig. 4. These results are all consistent with existing data (where available) and can be tested with future measurements.

*Hard and soft transport properties in sQGMP model.*—

We now present the details for computing the transport coefficients shown in Fig.1 and 2. The jet transport coefficient  $\hat{q}$  in CUJET3.0 can be computed from:

$$\hat{q}_F = \int_0^{6ET} dq^2 \frac{2\pi q^2}{(q^2 + f_E^2 \mu^2)(q^2 + f_M^2 \mu^2)} \rho(T) \times [(C_{qq} f_q + C_{qg} f_g) \alpha_s^2(q^2) + C_{qm}(1 - f_q - f_g)] . \quad (8)$$

The total number density  $\rho(T)$  is related to the lattice pressure  $p(T)$  s95p-PCE using  $\rho(T) = \xi p(T)/T$  with  $\xi = [90\zeta(3)(16 + 9N_f)]/[\pi^4(16 + 10.5N_f)] = 1.012$  for a  $N_c =$

3,  $N_f = 2.5$  SB gas. The  $\rho(T)$  here is identical to  $n(T(\mathbf{z}))$  in Eq. (1). The  $f_{q,g}$  are fractional quasi-parton densities of quark or gluon type which are parametrized via:  $f_q = c_q L(T)$ ,  $f_g = c_g L(T)^2$  with the same  $c_{q,g}$  and  $L(T)$  as in Eq. (6) and Fig.3. The monopole fraction is thus  $f_m(T) = 1 - f_q(T) - f_g(T)$ . The color factors in Eq.(8) are given by  $C_{qq} = \frac{4}{9}$ ,  $C_{gg} = C_{mm} = \frac{9}{4}$ ,  $C_{qg} = C_{gm} = C_{mq} = 1$ . Fig. 2 shows the  $\hat{q}_F$  for quark jets corresponding to CUJET3.0 with  $(\alpha_c, c_m) = (0.95, 0.3)$ . The results are compared with those from HTL-pQCD-based CUJET2.0 [45] with  $(\alpha_{max}, f_E, f_M) = (0.39, 1, 0)$ , as well as those from AdS/CFT calculations ( $\hat{q} \approx 26.69 \sqrt{\lambda/4\pi} T^3$  [46]). The  $\hat{q}/T^3$  shows a prominent peak around  $T_c$  as proposed in [41]. The absolute magnitude of  $\hat{q}$  in sQGMP demonstrates a smooth crossover from the weakly coupled pQCD limit well above  $T_c$  to the strongly coupled  $\mathcal{N} = 4$  super Yang-Mills (SYM) limit near  $T_c$ .

We now turn to the shear viscosity that can be ultimately connected with jet transport property in the weak coupling limit, as first pointed out in [6]. Following [4–6], an estimate of shear viscosity per entropy density  $\eta/s$  can be derived from kinetic theory:

$$\begin{aligned} \eta/s &= \frac{1}{s} \frac{4}{15} \sum_a \rho_a \langle p \rangle_a \lambda_a^{tr} \\ &= \frac{4T}{5s} \sum_a \rho_a \left( \sum_b \rho_b \int_0^{\langle S_{ab} \rangle/2} dq^2 \frac{4q^2}{\langle S_{ab} \rangle} \frac{d\sigma_{ab}}{dq^2} \right)^{-1} \\ &= \frac{18T^3}{5s} \sum_a \rho_a / \hat{q}_a(T, E = 3T) . \end{aligned} \quad (9)$$

Notice here we extrapolate  $\hat{q}(T, E)$  down to the average thermal energy scale  $E \sim 3T$  and denote  $\rho_a(T)$  as the quasi-parton density of type  $a = q, g, m$ . The mean thermal Mandelstam variable  $\langle S_{ab} \rangle \sim 18T^2$ . The contributions of  $a = q, g, m$  to  $\eta/s$  are shown in Fig. 1(a), with the fractions of quasi-parton densities shown in Fig. 1(b). The  $\hat{q}_{a=g,m}$  for adjoint gluons and monopoles are similar to Eq. (8), subject to appropriate changes of the color factors  $C_{ab}$ . For the case of monopole-monopole scattering the  $C_{mm}(1 - \chi_T)$  term is enhanced by  $1/\alpha^2(q)$  while  $\alpha^2(q^2) \rightarrow 1$  for the  $m + q$  and  $m + g$  channels. Clearly the viscosity of the system is dominated by the quark component which has the largest  $\rho_a/\hat{q}_a$ . Interestingly the  $\hat{q}/T^3$  enhancement in the 1-2  $T_c$  region due to quark-monopole scattering also reduces the  $\eta/s$  greatly and quickly relative to perturbative values at high temperature. A similar effect, i.e. the reduction of  $\eta/s$  due to enhanced gluon scattering rate by monopoles, was found earlier in [81] for a pure-gluon plasma. Toward  $T_c$  and below, monopoles will condense into vacuum and hadronic resonance gases shall take over the thermal system. Including such a hadronic component, as we will study in the future, is necessary for a more accurate description of a likely rapidly increasing  $\eta/s$  in the low-T region, as indicated by e.g. a recent work [82].

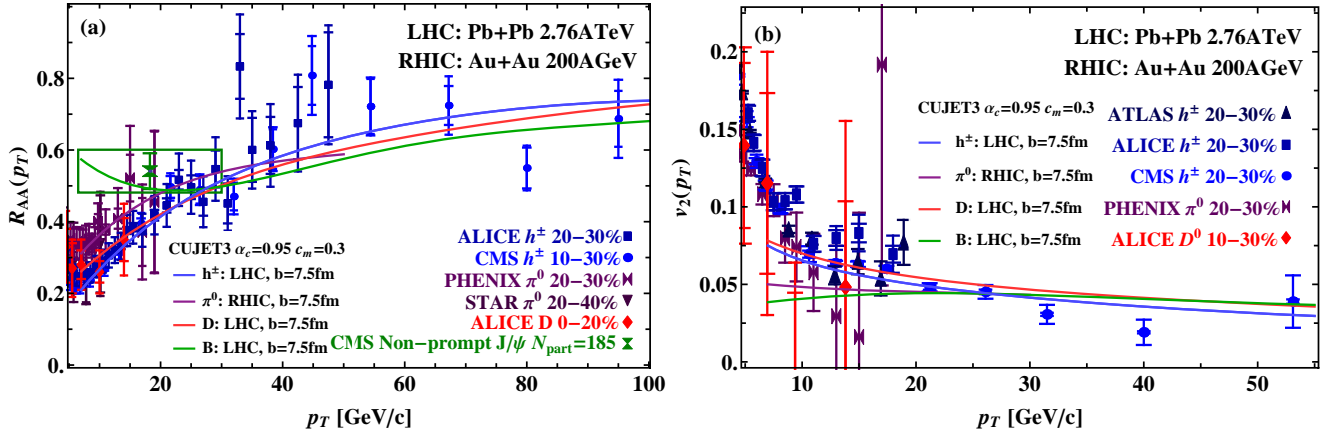


FIG. 4. (Color online) (a)  $R_{AA}(p_T)$  and (b)  $v_2(p_T)$  of inclusive neutral pions ( $\pi^0$ ) and charged particles ( $h^\pm$ ) in Au+Au  $\sqrt{s_{NN}} = 200$  GeV and Pb+Pb  $\sqrt{s_{NN}} = 2.76$  TeV collisions, computed from CUJET3.0 with the impact parameter  $b = 7.5$  fm, compared with corresponding data from ALICE, ATLAS, CMS, PHENIX and STAR [67–75]. With  $(\alpha_c, c_m) = (0.95, 0.3)$ , the results of CUJET3.0 are consistent with data of both  $R_{AA}$  and  $v_2$  at both RHIC and LHC simultaneously. CUJET3.0 ( $b = 7.5$  fm) predictions of  $R_{AA}(p_T)$  and  $v_2(p_T)$  for open heavy flavors (D meson, red; B meson, green) at LHC semi-peripheral Pb+Pb  $\sqrt{s_{NN}} = 2.76$  TeV collisions are also plotted. The D meson results with  $p_T < 20$  GeV/c agree with ALICE data of both  $R_{AA}$  and  $v_2$  [76, 77], while the B meson  $R_{AA}$  results at  $6.5 < p_T < 30$  GeV/c are in agreement with non-prompt  $J/\psi$  at CMS [78].

*Summary.* We have developed a jet energy loss framework CUJET3.0, based on the semi-quark-gluon-monopole plasma (sQGMP) model that implements non-perturbative effects constrained by lattice QCD data. This model leads to several highly nontrivial findings: a consistent description of both bulk perfect fluidity and high  $p_T$  jet quenching phenomena; a strong increase of  $\hat{q}/T^3$  accompanied by a strong decrease of  $\eta/s$  toward  $T_c$ ; a simultaneous description of high  $p_T$   $R_{AA}$  and  $v_2$  data at RHIC and the LHC. Potential modeling uncertainties have been checked [83] and these findings remain robust. More detailed results and discussions on this novel development will be reported in a forthcoming publication.

We thank Peter Petreczky for helpful discussions. The research of JX and MG is supported by U.S. DOE Nuclear Science Grants No. DE-FG02-93ER40764. The research of JL is supported by the National Science Foundation (Grant No. PHY-1352368). JL is also grateful to the RIKEN BNL Research Center for partial support.

\* xjc@phys.columbia.edu

† liaoji@indiana.edu

‡ gyulassy@phys.columbia.edu

- [1] M. Gyulassy and L. McLerran, Nucl. Phys. A **750**, 30 (2005).
- [2] E. V. Shuryak, Nucl. Phys. A **750**, 64 (2005).
- [3] B. Muller, J. Schukraft, and B. Wyslouch, Ann. Rev. Nucl. Part. Sci. **62**, 361 (2012).
- [4] P. Danielewicz and M. Gyulassy, Phys. Rev. D **31**, 53 (1985).
- [5] T. Hirano and M. Gyulassy, Nucl. Phys. A **769**, 71 (2006).
- [6] A. Majumder, B. Muller, and X. N. Wang, Phys. Rev. Lett. **99**, 192301 (2007).

- [7] H. Song and U. W. Heinz, Phys. Rev. C **78**, 024902 (2008).
- [8] C. Shen, U. Heinz, P. Huovinen, and H. Song, Phys. Rev. C **82**, 054904 (2010).
- [9] C. Gale, S. Jeon, B. Schenke, P. Tribedy and R. Venugopalan, Phys. Rev. Lett. **110**, no. 1, 012302 (2013).
- [10] K. M. Burke *et al.* (JET Collaboration), Phys. Rev. C **90**, no. 1, 014909 (2014).
- [11] R. Baier, D. Schiff, and B. Zakharov, Ann. Rev. Nucl. Part. Sci. **50**, 37 (2000).
- [12] M. Gyulassy, I. Vitev, X.-N. Wang, and B.-W. Zhang, arXiv:nucl-th/0302077.
- [13] A. Kovner and U. A. Wiedemann, arXiv:hep-ph/0304151.
- [14] P. Jacobs and X.-N. Wang, Prog. Part. Nucl. Phys. **54**, 443 (2005).
- [15] N. Armesto, B. Cole, C. Gale, W. A. Horowitz, P. Jacobs, et al., Phys. Rev. C **86**, 064904 (2012).
- [21] J. Casalderrey-Solana, H. Liu, D. Mateos, K. Rajagopal, and U. A. Wiedemann, arXiv:1101.0618.
- [17] W. Horowitz and M. Gyulassy, Nucl. Phys. A **872**, 265 (2011).
- [18] X. Zhang and J. Liao, Phys. Rev. C **89**, 014907 (2014).
- [19] X. Zhang and J. Liao, Phys. Rev. C **87**, 044910 (2013).
- [20] H. Liu, K. Rajagopal, and U. A. Wiedemann, J. High Energy Phys. **0703**, 066 (2007).
- [21] J. Casalderrey-Solana, H. Liu, D. Mateos, K. Rajagopal and U. A. Wiedemann, arXiv:1101.0618 [hep-th].
- [22] Y. Hidaka and R. D. Pisarski, Phys. Rev. D **78**, 071501 (2008).
- [23] Y. Hidaka and R. D. Pisarski, Phys. Rev. D **81**, 076002 (2010).
- [24] A. Dumitru, Y. Guo, Y. Hidaka, C. P. K. Altes, and R. D. Pisarski, Phys. Rev. D **83**, 034022 (2011).
- [25] S. Lin, R. D. Pisarski, and V. V. Skokov, Phys. Lett. B **730**, 236 (2014).
- [26] J. Liao and E. Shuryak, Phys. Rev. C **75**, 054907 (2007).
- [27] J. Liao and E. Shuryak, Phys. Rev. Lett. **101**, 162302 (2008).



- (2008).
- [28] J. Liao and E. Shuryak, Phys. Rev. Lett. **109**, 152001 (2012), 1206.3989.
  - [29] T. Renk, H. Holopainen, U. Heinz, and C. Shen, Phys. Rev. C **83**, 014910 (2011).
  - [30] A. Bazavov et al. (HotQCD Collaboration), arXiv:1407.6387.
  - [31] G. S. Bali, Phys. Rept. **343**, 1 (2001).
  - [32] G. Ripka, arXiv:hep-ph/0310102.
  - [33] K.-I. Kondo, S. Kato, A. Shibata, and T. Shinohara, arXiv:1409.1599.
  - [34] A. D'Alessandro and M. D'Elia, Nucl. Phys. B **799**, 241 (2008).
  - [35] A. D'Alessandro, M. D'Elia, and E. V. Shuryak, Phys. Rev. D **81**, 094501 (2010).
  - [36] C. Bonati and M. D'Elia, Nucl. Phys. B **877**, 233 (2013).
  - [37] M. N. Chernodub and V. I. Zakharov, Phys. Rev. Lett. **98**, 082002 (2007).
  - [38] B. Betz and M. Gyulassy, Phys. Rev. C **86**, 024903 (2012).
  - [39] M. Gyulassy, I. Vitev, and X. N. Wang, Phys. Rev. Lett. **86**, 2537 (2001).
  - [40] J. Jia and R. Wei, Phys. Rev. C **82**, 024902 (2010).
  - [41] J. Liao and E. Shuryak, Phys. Rev. Lett. **102**, 202302 (2009).
  - [42] B. Betz and M. Gyulassy, arXiv:1305.6458.
  - [43] B. Betz and M. Gyulassy, JHEP **1408**, 043 (2014) [Erratum-ibid. **1410**, 090 (2014)].
  - [44] D. Li, J. Liao, and M. Huang, Phys. Rev. D **89**, 126006 (2014).
  - [45] J. Xu, A. Buzzatti, and M. Gyulassy, J. High Energy Phys. **1408**, 063 (2014).
  - [46] H. Liu, K. Rajagopal, and U. A. Wiedemann, Phys. Rev. Lett. **97**, 182301 (2006).
  - [47] M. Gyulassy and X.-N. Wang, Nucl. Phys. B **420**, 583 (1994).
  - [48] M. Gyulassy, P. Levai, and I. Vitev, Nucl. Phys. B **594**, 371 (2001).
  - [49] M. Djordjevic and M. Gyulassy, Nucl. Phys. A **733**, 265 (2004).
  - [50] A. Buzzatti and M. Gyulassy, Phys. Rev. Lett. **108**, 022301 (2012).
  - [51] A. Buzzatti and M. Gyulassy, Nucl. Phys. A **904-905**, 779c (2013).
  - [52] M. Djordjevic and U. W. Heinz, Phys. Rev. Lett. **101**, 022302 (2008).
  - [53] R. Baier, A. Mueller, and D. Schiff, Phys. Lett. B **649**, 147 (2007).
  - [54] T. Renk, Phys. Rev. C **89**, 067901 (2014).
  - [55] A. Peshier, arXiv:hep-ph/0601119.
  - [56] B. Zakharov, JETP Lett. **88**, 781 (2008).
  - [57] L. Randall, R. Rattazzi, and E. V. Shuryak, Phys. Rev. D **59**, 035005 (1999).
  - [58] A. Bazavov, T. Bhattacharya, M. Cheng, N. Christ, C. DeTar, et al., Phys. Rev. D **80**, 014504 (2009).
  - [59] S. Borsanyi et al. (Wuppertal-Budapest Collaboration), J. High Energy Phys. **1009**, 073 (2010).
  - [60] A. Nakamura, T. Saito, and S. Sakai, Phys. Rev. D **69**, 014506 (2004).
  - [61] M. H. Thoma and M. Gyulassy, Nucl. Phys. B **351**, 491 (1991).
  - [62] X.-N. Wang, Private Communication.
  - [63] M. Cacciari, P. Nason, and R. Vogt, Phys. Rev. Lett. **95**, 122001 (2005).
  - [64] R. Glauber and G. Matthiae, Nucl. Phys. B **21**, 135 (1970).
  - [65] B. A. Kniehl, G. Kramer, and B. Potter, Nucl. Phys. B **582**, 514 (2000).
  - [66] C. Peterson, D. Schlatter, I. Schmitt, and P. M. Zerwas, Phys. Rev. D **27**, 105 (1983).
  - [67] A. Adare et al. (PHENIX Collaboration), Phys. Rev. Lett. **101**, 232301 (2008).
  - [68] A. Adare et al. (PHENIX Collaboration), Phys. Rev. Lett. **105**, 142301 (2010).
  - [69] A. Adare et al. (PHENIX Collaboration), Phys. Rev. C **87**, 034911 (2013).
  - [70] B. Abelev et al. (STAR Collaboration), Phys. Rev. C **80**, 044905 (2009).
  - [71] B. Abelev et al. (ALICE Collaboration), Phys. Lett. B **719**, 18 (2013).
  - [72] B. Abelev et al. (ALICE Collaboration), Phys. Lett. B **720**, 52 (2013).
  - [73] G. Aad et al. (ATLAS Collaboration), Phys. Lett. B **707**, 330 (2012).
  - [74] S. Chatrchyan et al. (CMS Collaboration), Eur. Phys. J. C **72**, 1945 (2012).
  - [75] S. Chatrchyan et al. (CMS Collaboration), Phys. Rev. Lett. **109**, 022301 (2012).
  - [76] B. Abelev et al. (ALICE Collaboration), JHEP **1209**, 112 (2012).
  - [77] B. B. Abelev et al. (ALICE Collaboration), Phys. Rev. C **90**, 034904 (2014).
  - [78] CMS Collaboration (CMS Collaboration), CMS-PAS-HIN-12-014.
  - [79] A. Bazavov, H.-T. Ding, P. Hegde, F. Karsch, C. Miao, S. Mukherjee, P. Petreczky, C. Schmidt, and A. Velytsky, Phys. Rev. D **88**, no. 9, 094021 (2013).
  - [80] S. Borsanyi, Z. Fodor, S. D. Katz, S. Krieg, C. Ratti, and K. Szabo, J. High Energy Phys. **1201**, 138 (2012).
  - [81] C. Ratti and E. Shuryak, Phys. Rev. D **80**, 034004 (2009).
  - [82] N. Christiansen, M. Haas, J. M. Pawłowski and N. Strodthoff, arXiv:1411.7986 [hep-ph].
  - [83] For example it could be possible that quarks are “liberated” more rapidly than Polyakov loop estimate Eq. (6). One may e.g. use lattice results on quark number susceptibilities [79, 80] to estimate the quark number densities. We have done the calculation with such prescription, which is found not to alter our main conclusions.